EKSPLOATACJA I NIEZAWODNOŚĆ
MAINTENANCE AND RELIABILITY

Eksploatacja i Niezawodnosc – Maintenance and Reliability

Volume 23 (2021), Issue 4

journal homepage: http://www.ein.org.pl

Article citation info:
Lyu H, Wang S, Zhang X, Yang Z, Pecht M. Reliability modeling for dependent competing failure processes with phase-type distribution considering changing degradation rate. Eksploatacja i Niezawodnosc – Maintenance and Reliability 2021; 23 (4): 627–635, http://doi.org/10.17531/ein.2021.4.5.

Reliability modeling for dependent competing failure processes with phase-type distribution considering changing degradation rate

Indexed by: Web of Science Group

Hao Lyu[a], Shuai Wang[a], Xiaowen Zhang[a], Zaiyou Yang[a], Michael Pecht[b]

[a]Northeastern University, School of Mechanical Engineering and Automation, Shenyang 110819, China
[b]University of Maryland, Center for Advanced Life Cycle Engineering, College Park, MD 20742, USA

Highlights

- The degradation rate changes when the number of shocks reaches a specific value.
- The phase-type (PH) distribution is combined with the DCFP.
- The survival function of PH distribution is used to calculate hard failure reliability.
- The phase-type distribution method is applied to calculate the reliability of the MEMS.

Abstract

In this paper, a system reliability model subject to Dependent Competing Failure Processes (DCFP) with phase-type (PH) distribution considering changing degradation rate is proposed. When the sum of continuous degradation and sudden degradation exceeds the soft failure threshold, soft failure occurs. The interarrival time between two successive shocks and total number of shocks before hard failure occurring follow the continuous PH distribution and discrete PH distribution, respectively. The hard failure reliability is calculated using the PH distribution survival function. Due to the shock on soft failure process, the degradation rate of soft failure will increase. When the number of shocks reaches a specific value, degradation rate changes. The hard failure is calculated by the extreme shock model, cumulative shock model, and run shock model, respectively. The closed-form reliability function is derived combining with the hard and soft failure reliability model. Finally, a Micro-Electro-Mechanical System (MEMS) demonstrates the effectiveness of the proposed model.

Keywords

dependent competing failure processes; phase-type distribution; changing degradation rate; reliability modeling; survival function..

Notation

$X(t)$	Continuous degradation at time t
$S(t)$	Cumulative degradation due to random shocks at time t
$X_S(t)$	Total degradation at time t
$N(t)$	Number of random shocks arrived by time t
λ	Intensity of random shocks
φ	Initial degradation
β_1	Initial degradation rate
β_2	Changed degradation rate when the number of shocks reaches a specific value
H	Soft failure threshold
D_1	Hard failure threshold under extreme shock model
D_2	Hard failure threshold under cumulative shock model
W_L	Critical level on shock magnitude under run shock model
W_U	Hard failure threshold under run shock model
W_i	The magnitude of the ith shock
$F_W(w)$	Cumulative distribution function (cdf) of W_i
Y_i	Degradation damage caused by the ith shock
T_j	Arrival time of the jth shock($T_j \sim$ Ga(j,λ))
J	The required number of shocks' occurrences when the soft failure degradation rate changes
k	The required number of consecutive shocks that exceed the critical level W_L under run shock model
N	The number of transfers before the Markov chain enters the absorption state
m	The maximum number of shocks that the system can support

1. Introduction

Many systems will fail due to various failure modes caused by degradation and random external shocks (such as wear, corrosion, fatigue, fracture, and shock loads) during operation [1]. Some systems may suffer multiple failure processes, and any failure processes will cause the system to fail. In this paper, we consider two failure processes: soft failure process and hard failure process. Soft failure means that the performance of the system gradually decreases over time. The system will fail when the degradation performance exceeds a certain critical threshold. Common soft failure includes wear, corrosion, and so forth. Hard failure refers to the phenomenon that the system breaks

E-mail addresses: H. Lyu - lvhao@me.neu.edu.cn, S. Wang - 2604150051@qq.com, X. Zhang - 15804042618@163.com, Z. Yang - 1171369333@qq.com, M. Pecht - pecht@umd.edu

down suddenly in the normal working process (e.g., fracture). These two failure processes compete because any failure will cause the system to fail [15]. Besides, because the shock acts on the soft and hard failure processes simultaneously, the soft and hard failure processes are dependent. It is challenging to predict system reliability when the soft and hard failure processes are dependent [25].

Most of researchers are devoted to the reliability prediction of systems that experience degradation or random shocks in the available literature. When there is not enough failure data, the degradation modeling method can indirectly provide the failure information of the system [25]. There are two main types of degradation models: the stochastic process model, such as the Wiener process, Gamma process, and inverse Gaussian process; and the other is the general path model [30]. Ni [21] developed degradation model for a two-stage degradation system subject to shocks, where degradation damage is caused by shocks and follows the Gamma distribution. The general path model is first introduced into the degradation literature by Lu and Meeker [16]. Because it is easy to use and the theory has been well established, the general path model has been used in many DCFP models to describe the degradation process [1, 6, 23, 25]. In our study, in order to implement the idea that the degradation rate changes when the number of shocks reaches a specific value, we use the general path model as the degradation process. Because the degradation rate in the general path model can be changed, this characteristic is exactly consistent with our idea. At the same time, the random shock model has been extensively studied. Various shock models are introduced into the hard failure reliability calculation. Shock models can be divided into the following categories: extreme shock model [29], cumulative shock model [20], run shock model [18], m shock model [11], delta shock model [13], and mixed shock model [26]. In this paper, hard failure is calculated under three different shock patterns: the extreme shock model, the cumulative shock model, and the run shock model.

In the available literature, most of the literature has been devoted to the reliability modeling subject to DCFP. Peng [23] developed reliability modeling for complex systems subject to multiple dependent competing failure processes, where two correlated failure processes are considered. Soft failure is caused jointly by continuous degradation and additional abrupt degradation damage due to a shock process and hard failure caused by abrupt stress from the same shock process. Guo [7] presented a joint copula reliability model for systems experiencing two degradation processes and random shocks, where the dependence between the two degradation processes is considered by copula function. Keedy [12] built a probabilistic reliability model for stents experiencing dependent competing risk processes. Crack propagation is regarded as a degradation process, and a single overload under external shocks is considered a hard failure process. Besides, shocks will accelerate the propagation of cracks, thus forming a dependent competing failure process. Huynh [10] proposed a Degradation-Threshold-Shock model with dependent competing failure modes, where the shock arrival rate follows the nonhomogeneous Poisson process, and the Poisson intensity depends on the degradation level of the system. Jiang [11] established reliability models for systems subject to multiple s-dependent competing failure processes. When the shock meets a particular random shock pattern, the hard failure threshold reduces to a lower level. Rafiee [25] investigated reliability models for a system subject to DCFP of degradation and random shocks with a changing degradation rate according to particular random shock patterns. Lin [14] and Hao [8] studied the general dependences between the degradation and two types of random shocks (extreme shocks and cumulative shocks). Fan [6] established a new reliability model for DCFP, where the intensity function of nonhomogeneous Poisson process depends on the degradation processes. Rafiee [26] investigated reliability modeling for systems subject to DCFP considering the impact of a new generalized mixed shock model. When the generalized mixed shock model is satisfied, the degradation rate and the hard failure threshold can simultaneously shift. Zhang [31] proposed a new reliability model for systems with multiple components subject to multiple natural degradations and random shocks, where the degradation rate will accelerate due to shocks. Che [4] studied a novel reliability model for load-sharing k-out-of-n systems, where the dependent workload and shock effects are considered. An [1] considered that systems with high reliability and long life could resist small shocks, and divided shocks into safety shocks, damage shocks, and fatal shocks, and carried out reliability modeling for multiple degradation and shock processes. Lyu [17] applied the reliability model of DCFP to the Turbine and Worm System. Pourhassan [24] put forward a simulation approach about analytic reliability assessment for complicated systems, which embeds the stochastic degradation process and random shocks. In most of the above literature, the interference model is utilized to calculate the hard failure reliability; that is, the system is reliable when the shock magnitude and shock times are less than a certain threshold or the interarrival shock time exceeds a certain threshold. In our research, the phase-type distribution method is employed to calculate the hard failure reliability. The interarrival time between two successive shocks is assumed to be continuous phase-type distribution, and the phase-type distribution survival function is used to calculate the reliability.

The phase-type distribution is suitable for modeling the interarrival time between two successive shocks. There are many advantages about the phase-type distribution method. First, the simplicity of mathematics is one of the advantages of the phase-type distribution method. We can express the distribution and moment in the form of matrix, and it is easy to calculate the results we need [22]. Second, When multiple shock sources act on a system, especially complex shocks such as run shocks, it is difficult to obtain a closed reliability expression with traditional hard failure reliability calculation methods, but the phase-type distribution method is easy to calculate the hard failure reliability. Besides, the closure properties of phase-type distributions under some operations are helpful in the reliability context [2]. In the literature [3, 19, 27], the phase-type distribution is applied to analyze the reliability of shock models. In the literature [3, 19], the interarrival time between shocks is assumed to be continuous phase-type distribution. Shocks may lead to system failure, and the system may fail due to wear. Its wear lifetime follows the continuous phase-type distribution. The interval between shocks and the wear life depend on the number of cumulative shocks. When the shocks are extreme shocks, cumulative shocks, and run shocks, the survival function of the system is obtained. Segovia [27] displayed an analytical expression of the survival function of a multi-state system that suffered shocks by using phase-type distribution. Zhao [32] proposed a multi-state shock model, where the Markov chain was constructed by the number of shocks of different types of shocks. When the interarrival time between shocks follows the common continuous phase-type distribution, the survival function and mean residual lifetime of the multi-state system were derived. Eryilmaz [5] developed a new mixed shock model, which combined the extreme shock model and the run shock model. The survival function of the system was studied when the interarrival time and the shock magnitude are independent and dependent using the property of phase-type distribution. The above literature used the phase-type distribution calculation method when calculating the failure reliability caused by shocks. Literature [3, 19, 27] assumed that the wear life follows a continuous phase-type distribution. When the failure is caused by wear, the survival function is used to describe the reliability of the system.

In the existing literature, the phase-type distribution calculation method has not been combined with DCFP. We combine the phase-type distribution calculation method with DCFP. As far as the author's knowledge, this is the first time for the research in combining phase-type distribution with DCFP. In this paper, the general path model is utilized for the soft failure. The degeneration path is assumed to be a linear path. The degradation rate changes when the number of shocks reaches a specific value. The soft failure reliability is calculated by the total degradation-threshold interference model. The phase-type distribution method is applied to calculate the hard failure. It is assumed that the interarrival time between shocks follows the common phase-type distribution, the total number of shocks before the hard failure occurring follows the discrete phase-type distribution, and the survival function is employed to calculate the hard failure reliability. The total reliability of the system is derived considering the hard and soft failures by the number of shocks.

The rest of this article is organized as follows. In Section 2, the soft failure process and the hard failure process of the system are described, along with the dependent competing failure relationship between those processes. In Section 3, the reliability models of the system, including the soft failure model, the hard failure model(the extreme shock model, cumulative shock model, and run shock model), and the model of DCFP, are established. In Section 4, a numerical example is developed to demonstrate the implementation and effectiveness of the proposed model. In Section 5, the calculation results are summarized.

2. System description and preliminaries

As shown in Figure 1, the failure of a system is caused by two dependent competing failure processes: the soft failure process and the hard failure process. The total degradation of the soft failure process consists of continuous degradation and sudden degradation caused by shocks. When the total degradation exceeds the soft failure threshold H, soft failure occurs in the system. At the same time, hard failure will occur when the shock magnitude exceeds the hard failure threshold D. Whichever failure processes occurs first will cause the system to fail. The shock process acts on the soft and hard failure process simultaneously, so system failure results from dependent competing failures in the soft and hard failure process. In this paper, three shock models are applied for the hard failure process: (1) Extreme shock model, when the shock magnitude exceeds the hard failure threshold, the system will have a hard failure. (2) Cumulative shock model, when the cumulative magnitude of shocks exceeds the hard failure threshold, hard failure occurs in the system. (3) Run shock model, when the magnitude of k consecutive shocks exceeds the critical threshold, hard failure occurs. Besides, when the number of shocks reaches a certain value, the degradation rate of soft failure changes.

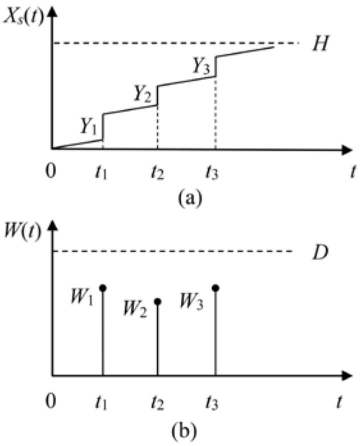

Fig. 1. Two dependent competing failure processes: (a) soft failure, (b) hard failure

Phase-type distributions and property:

Consider a finite discrete-time Markov chain in the state space {1, 2, ..., m, m+1}, where 1, 2, ..., m are the transient states, and m+1 is the absorbing state. The number of transitions before the Markov chain enters the absorbing state is defined as a discrete phase-type distribution. The probability mass function of discrete phase-type distributed random variable N is [22]:

$$P\{N=n\}=\mathbf{a}\mathbf{Q}^{n-1}\mathbf{u}', \quad n=1,2,\cdots \tag{1}$$

where, for $n\in\mathbf{N}$, $\mathbf{Q}=(q_{ij})_{m\times m}$ is the transition probability matrix between m transient states, and $\mathbf{u}'=(\mathbf{I}-\mathbf{Q})\mathbf{e}'$ is the transition probability vector from the transient state to the absorption state, $\mathbf{I}$ is the identity matrix. The matrix $\mathbf{Q}$ must satisfy the condition that $\mathbf{I}$-$\mathbf{Q}$ is non-singular. We use $N\sim PH_d(\mathbf{a},\mathbf{Q})$ to indicate that the random variable N follows the discrete phase-type distribution.

Assuming a finite-state Markov process starts the transition from transient state i with probability a_i. The time distribution of the Markov process entering the absorbing state is defined as continuous phase-type distribution. The cumulative distribution function of continuous phase-type distributed random variable X is [22]:

$$P(X\le x)=1-\boldsymbol{\alpha}\exp(\mathbf{A}x)\mathbf{e}' \tag{2}$$

The survival function of X is given by:

$$P(X>x)=\boldsymbol{\alpha}\exp(\mathbf{A}x)\mathbf{e}' \tag{3}$$

where, $\mathbf{A}$ is an m×m matrix, whose diagonal elements are negative, and non-diagonal elements are non-negative, and $\mathbf{e}=(1,\ldots,1)_{1\times m}$. All elements of the row vector $\boldsymbol{\alpha}=(a_1,\ldots,a_m)$ are non-negative. Exponential, Erlang, generalized Erlang, and Coxian distributions are commonly-used continuous phase-type distributions [9]. We use $X\sim PH_c(\boldsymbol{\alpha},\mathbf{A})$ to indicate that the random variable X follows the continuous phase-type distribution of order m with a PH-generator $\mathbf{A}$ and substochastic vector $\boldsymbol{\alpha}$.

Proposition [22]: Assume that X_1, X_2,… are independent and $X_i\sim PH_c(\boldsymbol{\alpha},\mathbf{A})$, i=1,2,… and independently $N\sim PH_d(\mathbf{a},\mathbf{Q})$. If $\boldsymbol{\alpha}$ and $\mathbf{a}$ are stochastic vectors, i.e., $\boldsymbol{\alpha}\mathbf{e}'=1, \mathbf{a}\mathbf{e}'=1$, then $\sum_{i=1}^{N}X_i\sim PH_c\left(\boldsymbol{\alpha}\otimes\mathbf{a},\mathbf{A}\otimes\mathbf{I}+\left(\mathbf{a}^0\boldsymbol{\alpha}\right)\otimes\mathbf{Q}\right),\ \mathbf{a}^0=-\mathbf{A}\mathbf{e}'$.

where ⊗ is the Kronecker product.

3. Reliability analysis of DCFP considering time phase-type distribution

In this section, the reliability analysis of the system experiencing the degradation process and the shock process is carried out. First, the soft failure model is developed—the degradation rate changes when the number of shocks reaches a specific value. Then the phase-type distribution is utilized to model the hard failure process (including extreme shock, cumulative shock, and run shock). Finally, the total reliability is calculated.

3.1. Soft failure model under degradation and random shocks

The total degradation includes continuous degradation and abrupt degradation caused by random shocks. The continuous degradation path is assumed to be a linear path $X(t)=\varphi+\beta t$. φ is the initial degradation, β_1 is the degradation rate of the first stage, β_2 is the degradation rate of the second stage. Assume that the initial degradation φ, the degradation rate β_1 and β_2 all follow the normal distribution, that is, $\beta_1\sim N(\mu_{\beta1},\sigma_{\beta1}^2)$, $\beta_2\sim N(\mu_{\beta2},\sigma_{\beta2}^2)$. The degradation rate changes when the jth shock arrives. Then the continuous degradation $X(t)$ can be expressed as:

$$X(t)=\begin{cases}\varphi+\beta_1 t, & j>N(t)\\ \varphi+\beta_1 T_j+\beta_2(t-T_j), & j\le N(t)\end{cases} \tag{4}$$

where, T_j is the time of arrival of the jth shock, and $N(t)$ is the number of random shocks arrived by time t.

Random shocks will cause abrupt degradation damage to the degradation process, thereby accelerating the degradation process. Assuming that the magnitude of the random shock W_i is independent and identically normally distributed, namely $W_i(t_i)\sim N(\mu_W, \sigma_W^2)$, t_i is the arrival time of the ith shock. The cumulative distribution function of the shock magnitude is $F_W(x)$. The arrival times of random shocks follow a homogeneous Poisson process with intensity λ, then:

$$P\{N(t)=i\}=\frac{(\lambda t)^i}{i!}e^{-\lambda t},\ \ i=0,1,2,\cdots \tag{5}$$

When the number of random shock arrivals follows the Poisson process with intensity λ, for a certain j, the arrival time T_j of the jth shock follows the Gamma distribution with shape parameter j and scale parameter λ, that is, $T_j\sim$ Ga(j,λ). The probability density function is:

$$f_{T_j}(t_j;j)=\frac{\lambda^j}{(j-1)!}t_j{}^{j-1}e^{-\lambda t_j} \tag{6}$$

Let Y_i (i=1,2,…,∞) be the abrupt degeneration increment caused by the ith random shock, that is, the damage caused by the random shock to the degradation process. Then the total degradation $S(t)$ caused by random shocks is:

$$S(t)=\begin{cases}\sum_{i=1}^{N(t)}Y_i, & N(t)>0\\ 0, & N(t)=0\end{cases} \tag{7}$$

Then the total degradation of soft failure Xs(t) can be expressed as:

$$X_S(t)=X(t)+S(t) \tag{8}$$

To keep the system in normal working condition, the total degradation of the system $X_s(t)$ should be less than the soft failure critical threshold H. The reliability of the soft failure is:

$$\begin{aligned}R_s(t)&=P\left(X_s(t)<H\right)=P\left(X(t)+S(t)<H\right)=P\left(X(t)+\sum_{i=1}^{N(t)}Y_i<H\right)\\
&=P\left(X(t)<H\mid N(t)=0\right)\cdot P\left(N(t)=0\right)+\sum_{i=1}^{\infty}P\left(X(t)+\sum_{i=1}^{N(t)}Y_i<H\mid N(t)=i\right)\cdot P\left(N(t)=i\right)\\
&=P\left(\varphi+\beta_1 t<H\right)\cdot P\left(N(t)=0\right)+\sum_{i=1}^{j}P\left(\varphi+\beta_1 t+\sum_{i=1}^{N(t)}Y_i<H\right)\cdot P\left(N(t)=i\right)\\
&+\sum_{i=j+1}^{\infty}P\left(\varphi+\beta_1 T_j+\beta_2(t-T_j)+\sum_{i=1}^{N(t)}Y_i<H\right)\cdot P\left(N(t)=i\right)\\
&=\Phi\left(\frac{H-(\varphi+\mu_{\beta_1}t)}{\sqrt{\sigma_{\beta_1}^2t^2}}\right)\cdot\exp(-\lambda t)+\sum_{i=1}^{j}\Phi\left(\frac{H-(\varphi+\mu_{\beta_1}t+i\mu_Y)}{\sqrt{\sigma_{\beta_1}^2t^2+i\sigma_Y^2}}\right)\cdot\frac{\exp(-\lambda t)(\lambda t)^i}{i!}\\
&+\sum_{i=j+1}^{\infty}\int_0^t\Phi\left(\frac{H-\left(\varphi+\mu_{\beta_1}t_j+\mu_{\beta_2}(t-t_j)+i\mu_Y\right)}{\sqrt{\sigma_{\beta_1}^2t_j{}^2+\sigma_{\beta_2}^2(t-t_j)^2+i\sigma_Y^2}}\right)\frac{\lambda^j}{(j-1)!}t_j^{j-1}e^{-\lambda t_j}dt_j\cdot\frac{\exp(-\lambda t)(\lambda t)^i}{i!}\end{aligned} \tag{9}$$

3.2. Hard failure model under extreme shock

The extreme shock model is shown in Figure 2. It can be seen from Figure 2 (a) that when the number of shocks reaches a specific value (the schematic diagram is 3), the soft failure degradation rate increases from β_1 to β_2. As shown in Figure 2(b), the fourth shock is a fatal shock, so the system life is T=X_1+X_2+X_3+X_4.

Let X_i denote the interarrival time between the ith shock and the i–1th shock, i≥1. Suppose the arrival rate of the shock follows a Poisson distribution with parameter λ. In that case, the interarrival time X_i follows the exponential distribution, which can be expressed as phase-type distribution:

$$X_i\sim PH_c(\boldsymbol{\alpha},\mathbf{A})=PH_c(1,-\lambda) \tag{10}$$

Let p_1 be the probability of a fatal shock, and 1–p_1 be the probability of a non-fatal shock.

$$p_1=P\left(W_i>D_1\right)=1-F_W\left(D_1\right)=1-\Phi\left(\frac{D-\mu_W}{\sigma_W}\right) \tag{11}$$

where $\Phi(\bullet)$ is the cumulative distribution function of standard normal distribution.

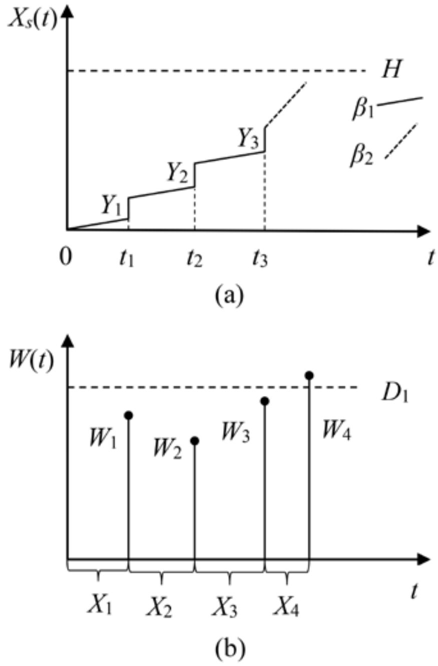

Fig. 2. Extreme shock model

Let N be the number of transfers before the Markov chain enters the absorption state, that is, the number of shocks before hard failure occurring, which follows the discrete phase-type distribution, namely $N\sim PH_d(\mathbf{a},\mathbf{Q})$

$$\mathbf{a}=\begin{pmatrix}1&0&0&0&\cdots&0\end{pmatrix}_{1\times(m+1)},\ \mathbf{Q}=\begin{pmatrix}0&1-p_1&0&\cdots&0\\0&0&1-p_1&\cdots&0\\0&0&0&\ddots&\vdots\\\vdots&\vdots&\vdots&\ddots&1-p_1\\0&0&0&\cdots&0\end{pmatrix}_{(m+1)\times(m+1)} \tag{12}$$

where, m is the maximum number of shocks that the system can support.

Let T be the life of the hard failure of the system, then according to the phase-type distribution properties, we have:

$$T=\sum_{i=1}^{N}X_i\sim PH_c(\mathbf{g},\mathbf{G})=PH_c\left(\pm\otimes\mathbf{a},\mathbf{A}\otimes\mathbf{I}+\left(\mathbf{a}^0\alpha\right)\otimes\mathbf{Q}\right),\ \ \mathbf{a}^0=-\mathbf{A}\mathbf{e}'$$

$$\mathbf{g}=\begin{pmatrix}1 & 0 & 0 & 0 & \cdots & 0\end{pmatrix}_{1\times(m+1)},\ \mathbf{G}=\begin{pmatrix}-\lambda & \lambda(1-p_1) & 0 & \cdots & 0\\ 0 & -\lambda & \lambda(1-p_1) & \cdots & 0\\ 0 & 0 & -\lambda & \ddots & \vdots\\ \vdots & \vdots & \vdots & \ddots & \lambda(1-p_1)\\ 0 & 0 & 0 & \cdots & -\lambda\end{pmatrix}_{(m+1)\times(m+1)} \tag{13}$$

According to the phase-type distribution survival function, we have:

$$P(T>t)=\mathbf{g}\exp(\mathbf{G}t)\mathbf{e}' \tag{14}$$

Because the soft failure reliability formula is derived by the number of shocks as the conditional probability, in order to unify the reliability expression of soft and hard failures, the hard failure reliability formula also uses the number of shocks as the conditional probability. Therefore, the hard failure reliability can be expressed as:

$$\begin{aligned}R_H(t)&=P(T>t)=\sum_{i=0}^{\infty}(T>t\mid N(t)=i)\cdot P(N(t)=i)\\&=\sum_{i=0}^{\infty}P(T>t)\cdot\frac{\exp(-\lambda t)(\lambda t)^i}{i!}=\sum_{i=0}^{\infty}\mathbf{g}\exp(\mathbf{G}t)\mathbf{e}'\cdot\frac{\exp(-\lambda t)(\lambda t)^i}{i!}\end{aligned} \tag{15}$$

3.3. Hard failure model under cumulative shock

The cumulative shock model is shown in Figure 3. It can be seen from Figure 3 (a) that when the number of shocks reaches a specific value (the schematic diagram is 3), the soft failure degradation rate increases from β_1 to β_2. As shown in Figure 3(b), the fourth cumulative shock exceeds the hard failure threshold, the system fails, so the system life is $T=X_1+X_2+X_3+X_4$.

Let p_i be the probability that the ith cumulative shock is a fatal shock, then:

$$p_i=1-\Phi\left(\frac{D_2-i\mu_W}{\sqrt{i\sigma_W^{\ 2}}}\right) \tag{16}$$

Let N be the number of transfers before the Markov chain enters the absorption state, which follows the discrete phase-type distribution, namely $N\sim PH_d(\mathbf{a},\mathbf{Q})$

$$\mathbf{a}=\begin{pmatrix}1 & 0 & 0 & 0 & \cdots & 0\end{pmatrix}_{1\times(m+1)},\ \mathbf{Q}=\begin{pmatrix}0 & 1-p_1 & 0 & \cdots & 0\\ 0 & 0 & 1-p_2 & \cdots & 0\\ 0 & 0 & 0 & \ddots & \vdots\\ \vdots & \vdots & \vdots & \ddots & 1-p_m\\ 0 & 0 & 0 & \cdots & 0\end{pmatrix}_{(m+1)\times(m+1)} \tag{17}$$

where, m is the maximum number of shocks that the system can support.

Let T be the life of the hard failure of the system, then according to the phase-type distribution properties, we have:

$$T=\sum_{i=1}^{N}X_i\sim PH_c(\mathbf{g},\mathbf{G})=PH_c\left(\pm\otimes\mathbf{a},\mathbf{A}\otimes\mathbf{I}+\left(\mathbf{a}^0\alpha\right)\otimes\mathbf{Q}\right),\ \mathbf{a}^0=-\mathbf{A}\mathbf{e}'$$

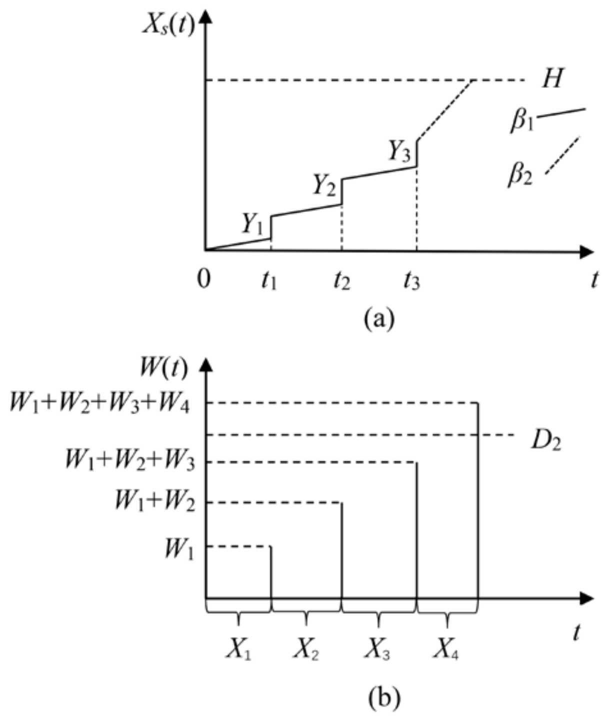

Fig. 3. Cumulative shock model

$$\mathbf{g}=\begin{pmatrix}1 & 0 & 0 & 0 & \cdots & 0\end{pmatrix}_{1\times(m+1)},\ \mathbf{G}=\begin{pmatrix}-\lambda & \lambda(1-p_1) & 0 & \cdots & 0\\ 0 & -\lambda & \lambda(1-p_2) & \cdots & 0\\ 0 & 0 & -\lambda & \ddots & \vdots\\ \vdots & \vdots & \vdots & \ddots & \lambda(1-p_m)\\ 0 & 0 & 0 & \cdots & -\lambda\end{pmatrix}_{(m+1)\times(m+1)} \tag{18}$$

According to the phase-type distribution survival function, we have $P(T>t)=\mathbf{g}\exp(\mathbf{G}t)\mathbf{e}'$

Therefore, the hard failure reliability can be expressed as:

$$\begin{aligned}R_H(t)&=P(T>t)=\sum_{i=0}^{\infty}(T>t\mid N(t)=i)\cdot P(N(t)=i)\\&=\sum_{i=0}^{\infty}P(T>t)\cdot\frac{\exp(-\lambda t)(\lambda t)^i}{i!}=\sum_{i=0}^{\infty}\mathbf{g}\exp(\mathbf{G}t)\mathbf{e}'\cdot\frac{\exp(-\lambda t)(\lambda t)^i}{i!}\end{aligned} \tag{19}$$

3.4. Hard failure model under run shock

The run shock model is shown in Figure 4. k=2 means that when the magnitude of two consecutive shocks exceeds the critical threshold W_L, hard failure occurs. It can be seen from Figure 4 (a) that when the number of shocks reaches a specific value (the schematic diagram is 3), the soft failure degradation rate increases from β_1 to β_2. As shown in Figure 4(b), when the fourth shock arrives, the condition of system failure caused by run shock is met, so the system life is $T=X_1+X_2+X_3+X_4$.

Let p represent the probability that the shock exceeds the critical level of run shock model under the condition that the shock is not fatal, then:

$$p=P(W_i>W_L\mid W_i<W_U)=\frac{P(W_L<W_i<W_U)}{P(W_i<W_U)}=\frac{F_W(W_U)-F_W(W_L)}{F_W(W_U)} \tag{20}$$

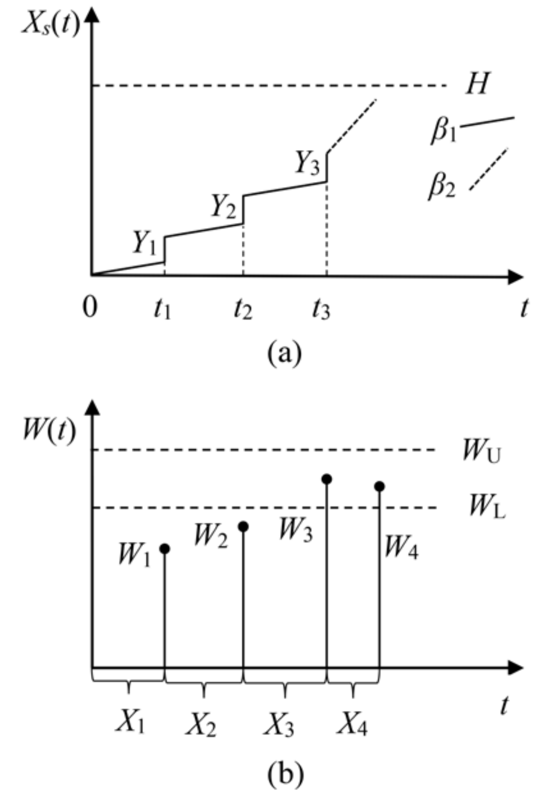

Fig. 4. Run shock model(k=2)

Let N be the number of transfers before the Markov chain enters the absorption state, which follows the discrete phase-type distribution, namely $N \sim PH_d(\mathbf{a},\mathbf{Q})$:

$$\mathbf{a} = \begin{pmatrix}1 & 0 & 0 & 0 & \cdots & 0\end{pmatrix}_{1\times k},\ \mathbf{Q} = \begin{pmatrix} 1-p & p & 0 & \cdots & 0 \\ 1-p & 0 & p & \cdots & 0 \\ 1-p & 0 & 0 & \ddots & \vdots \\ \vdots & \vdots & \vdots & \ddots & p \\ 1-p & 0 & 0 & \cdots & 0 \end{pmatrix}_{k\times k} \tag{21}$$

where, k is the required number of consecutive shocks that exceed the critical level W_L under run shock model.

Let T be the life of the hard failure of the system, then according to the phase-type distribution properties, we have:

$$T = \sum_{i=1}^{N} X_i \sim PH_c(\mathbf{g},\mathbf{G}) = PH_c\left(\boldsymbol{\alpha}\otimes\mathbf{a}, \mathbf{A}\otimes\mathbf{I} + \left(\mathbf{a}^0\boldsymbol{\alpha}\right)\otimes\mathbf{Q}\right),\ \ \mathbf{a}^0 = -\mathbf{A}\mathbf{e}'$$

$$\mathbf{g} = \begin{pmatrix}1 & 0 & 0 & 0 & \cdots & 0\end{pmatrix}_{1\times k},\ \mathbf{G} = \begin{pmatrix} -\lambda p & \lambda p & 0 & \cdots & 0 \\ \lambda(1-p) & -\lambda & \lambda p & \cdots & 0 \\ \lambda(1-p) & 0 & -\lambda & \ddots & \vdots \\ \vdots & \vdots & \vdots & \ddots & \lambda p \\ \lambda(1-p) & 0 & 0 & \cdots & -\lambda \end{pmatrix}_{k\times k} \tag{22}$$

According to the phase-type distribution survival function, we have $P(T>t) = \mathbf{g}\exp(\mathbf{G}t)\mathbf{e}'$

Therefore, the hard failure reliability can be expressed as:

$$R_H(t) = P(T>t) = \sum_{i=0}^{\infty}\left(T>t \mid N(t)=i\right)\cdot P\left(N(t)=i\right)$$
$$= \sum_{i=0}^{\infty} P(T>t)\cdot\frac{\exp(-\lambda t)(\lambda t)^i}{i!} = \sum_{i=0}^{\infty}\mathbf{g}\exp(\mathbf{G}t)\mathbf{e}'\cdot\frac{\exp(-\lambda t)(\lambda t)^i}{i!} \tag{23}$$

3.5. System reliability analysis

The system experiences both soft and hard failure processes at the same time. If the system is not to fail, neither soft nor hard failures can occur. According to Section 3.1 to 3.4, we have obtained the system's soft and hard failure reliability expressions. Therefore the total reliability is:

$$R(t) = P\left(X_s(t)<H, T>t\right) = P\left(X_s(t)<H, T>t \mid N(t)=0\right)\cdot P\left(N(t)=0\right)$$
$$+\sum_{i=1}^{\infty} P\left(X_s(t)<H,\ T>t \mid N(t)=i\right)\cdot P\left(N(t)=i\right)$$
$$= P\left(X(t)<H, T>t \mid N(t)=0\right)\cdot P\left(N(t)=0\right) + \sum_{i=1}^{\infty} P\left(X_s(t)<H,\ T>t \mid N(t)=i\right)\cdot P\left(N(t)=i\right)$$
$$= \Phi\left(\frac{H-(\varphi+\mu_{\beta_1}t)}{\sqrt{\sigma_{\beta_1}^2 t^2}}\right)\cdot\mathbf{g}\exp(\mathbf{G}t)\mathbf{e}'\cdot\exp(-\lambda t) + \sum_{i=1}^{j} P\left(\varphi+\beta_1 t + \sum_{i=1}^{N(t)} Y_i < H\right)\cdot P(T>t)\cdot P\left(N(t)=i\right)$$
$$+\sum_{i=j+1}^{\infty} P\left(\varphi+\beta_1 T_j + \beta_2(t-T_j) + \sum_{i=1}^{N(t)} Y_i < H\right)\cdot P(T>t)\cdot P\left(N(t)=i\right)$$
$$= \Phi\left(\frac{H-(\varphi+\mu_{\beta_1}t)}{\sqrt{\sigma_{\beta_1}^2 t^2}}\right)\cdot\mathbf{g}\exp(\mathbf{G}t)\mathbf{e}'\cdot\exp(-\lambda t) + \sum_{i=1}^{j}\Phi\left(\frac{H-(\varphi+\mu_{\beta_1}t+i\mu_Y)}{\sqrt{\sigma_{\beta_1}^2 t^2 + i\sigma_Y^2}}\right)\cdot\mathbf{g}\exp(\mathbf{G}t)\mathbf{e}'\cdot\frac{\exp(-\lambda t)(\lambda t)^i}{i!}$$
$$+\sum_{i=j+1}^{\infty}\int_0^t \Phi\left(\frac{H-\left(\varphi+\mu_{\beta_1}t_j+\mu_{\beta_2}(t-t_j)+i\mu_Y\right)}{\sqrt{\sigma_{\beta_1}^2 {t_j}^2 + \sigma_{\beta_2}^2(t-t_j)^2 + i\sigma_Y^2}}\right)\frac{\lambda^j}{(j-1)!}t_j^{j-1}e^{-\lambda t_j}dt_j\cdot\mathbf{g}\exp(\mathbf{G}t)\mathbf{e}'\cdot\frac{\exp(-\lambda t)(\lambda t)^i}{i!} \tag{24}$$

4. Numerical examples

In this section, a micro-engine is studied as a realistic example to illustrate the proposed model's effectiveness in this paper. The micro-engine includes comb-drive actuators and rotating gear, which are mechanically connected. After the voltage is applied, the comb-drive linear displacement is transformed into the circular motion of the gear through the pin joint. According to the experimental research conducted by Sandia National Laboratory, the wear of the friction surface between the gear and the cylindrical pin is the primary failure mode of the micro-engine, and the increase in wear eventually causes the cylindrical pin to break. The micro-engine is not only subjected to wear but also to random shocks. Tanner *et al.* [28] conducted a reliability analysis on the micro-engine in the shock environment. Random shocks will cause wear debris and accelerate the wear of the friction surface. Besides, under the impact of the shock, the spring may be misaligned, and a shock with sufficient magnitude may cause the spring to break. Because the shock will accelerate the degradation process, we assume that the degradation rate increases after the number of shocks reaches a specific value. The parameters used in reliability analysis are shown in Table 1.

The total reliability curves, soft failure reliability curves, and hard failure reliability curves under the extreme shock model, cumulative shock model, and run shock model are shown in Fig. 5. Besides, the sensitivity curves of (D_1, D_2, W_L), Poisson intensity λ, and soft failure degradation rate β_2 under three shock models are demonstrated in Fig. 6 – 8.

It can be seen from the soft failure reliability curve and the total reliability curve in Fig. 5 (a) that when t is around 0.8×10^5, the decline rate of the soft failure reliability curve and the total reliability curve becomes faster, which is because the number of shock arrivals reaches a certain threshold at this time. The soft failure degradation rate in-

Table 1. Parameter values of the reliability model

Parameters	Values	Sources
H	0.00125 μm^3	(Tanner&Dugger,2003)
D_1	1.5 GPa	(Rafiee, 2014)
D_2	5.0 Gpa	(Hao, 2017)
W_U W_L	1.8 Gpa 1.5 Gpa	Assumption (Rafiee, 2014)
φ	0	(Tanner&Dugger,2003)
$\mu_{\beta1}$	8.4823×10^{-9} μm^3	(Tanner&Dugger,2003)
$\sigma_{\beta1}$	6.0016×10^{-10} μm^3	(Tanner&Dugger,2003)
$\mu_{\beta2}$	10.4823×10^{-9} μm^3	(Rafiee, 2014)
$\sigma_{\beta2}$	6.0016×10^{-10} μm^3	(Tanner&Dugger,2003)
μ_W	1.2 GPa	(Rafiee, 2014)
σ_W	0.2 GPa	(Rafiee, 2014)
μ_Y	1.0×10^{-4} μm^3	(Rafiee, 2014)
σ_Y	2×10^{-5} μm^3	(Rafiee, 2014)
λ	5×10^{-5} / revolutions	(Rafiee, 2014)
j	3	Assumption
k	2	Assumption

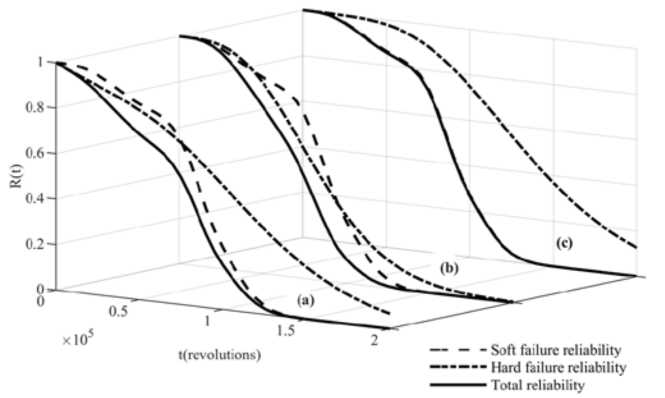

Fig. 5. Curves of soft failure reliability, hard failure reliability, and total reliability: (a) extreme shock model, (b) cumulative shock model, (c) run shock model

creases, resulting in a faster decline in soft failure reliability and total reliability. It can be seen from Fig. 6 (a) that when the hard failure threshold D_1 is increased from 1.3 to 1.6, the reliability curve shifts to the right. We have increased the hard failure threshold, and the system has better performance, which increases the hard failure reliability, and the total reliability becomes greater. It can be seen from Fig. 7 (a) that when the Poisson intensity λ increases, the reliability curve shifts to the left. We have increased the frequency of shock arrivals, and the system is in a worse working environment, thus reducing the reliability. It can be seen from Fig. 8 (a) that with the increase of β_2, the reliability curve shifts to the left, which is due to the increase in the rate of soft failure degradation leads to a decrease in the soft failure reliability, thereby reducing the total reliability.

It can be seen from Fig. 6 (b) that when the hard failure threshold D_2 increases from 4.0 to 7.0, the total reliability curve shifts to the right. As D_2 decreases, the inflection point of the total reliability curve becomes less noticeable. It is because when D_2 is a smaller value, the number of shocks required to cause the system to fail is small. The system will fail when the number of shocks has not reached a predetermined value that changes the degradation rate of soft failure, so the

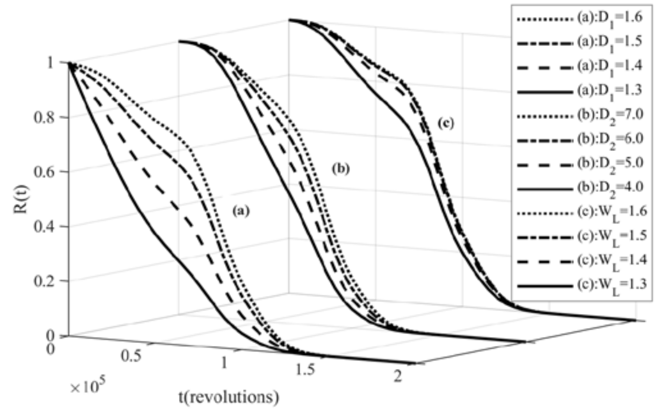

Fig. 6. Sensitivity analysis of R(t) on D_1, D_2, W_L: (a) extreme shock model, (b) cumulative shock model, (c) run shock model

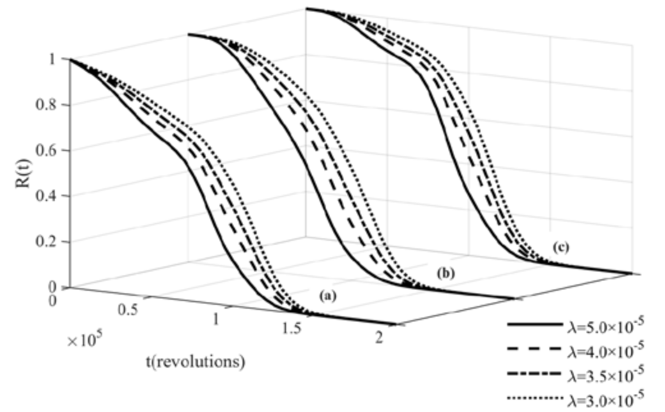

Fig. 7. Sensitivity analysis of R(t) on λ: (a) extreme shock model, (b) cumulative shock model, (c) run shock model

inflection point of the reliability curve is not apparent. It can be seen from Fig. 7 (b) that when the Poisson intensity λ increases, the reliability curve shifts more obviously to the left, which indicates that the reliability of the system is more sensitive to the frequency of shock arrival. So it is necessary to minimize the frequency of shock arrivals to maintain high reliability. It can be seen from Fig. 8 (b) that with the increase of β_2, the reliability curve shifts to the left. The rise of the soft failure degradation rate leads to a decrease in soft failure reliability, reducing the total reliability.

It can be seen from Fig. 5 (c) that compared with the total reliability under the extreme shock model (see Fig. 5 (a)), the total reliability under the run shock model is higher. It is because when the hard failure threshold under extreme shock model D_1 and the critical level on shock magnitude under run shock model W_L are the same, the run shock model requires that the system fails when two consecutive shocks exceed W_L, while the extreme shock model only needs one shock to exceed D_1. It can be seen from Fig. 6 (c) that when the critical level on shock magnitude W_L increases from 1.3 to 1.6, the total reliability curves are relatively close, which shows that the reliability of the system is less sensitive to the critical level on shock magnitude W_L. It can be seen from Fig. 7 (c) that when the Poisson intensity λ increases, the reliability curve shifts more obviously to the left, which indicates that the reliability of the system is more sensitive to the frequency of the shock. So it is necessary to minimize the frequency of shock arrivals to maintain high reliability. It can be seen from Fig. 8 (c) that with the increase of β_2, the reliability curve shifts to the left. It is due to the rise in the soft failure degradation rate, which leads to a decrease in the soft failure reliability and the total reliability.

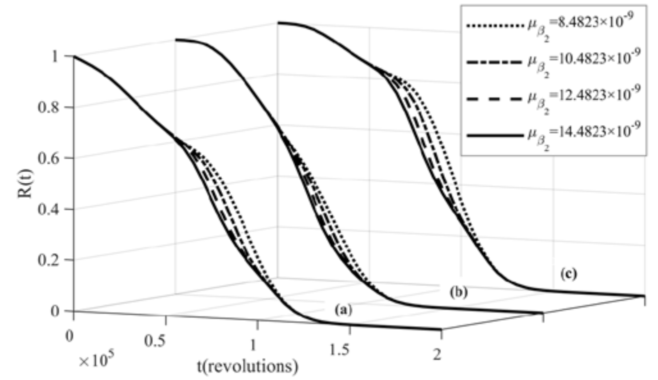

Fig. 8. Sensitivity analysis of R(t) on β_2: (a) extreme shock model, (b) cumulative shock model, (c) run shock model

5. Conclusions

In this paper, based on the phase-type distribution, we develop a new reliability model for systems subject to DCFP with phase-type distribution considering changing degradation rate. The main innovations of this paper are as follows: first, when the number of shocks reaches a specific value, the soft failure degradation rate changes; second, the phase-type distribution method is utilized to calculate the hard failure reliability—the interarrival time between two successive shocks follows a continuous phase-type distribution, and the survival function of the phase-type distribution is applied to calculate the hard failure reliability; third, the phase-type distribution is combined with the DCFP. Besides, the hard failure shock model adopts the extreme shock model, cumulative shock model, and run shock model, respectively. Finally, the proposed new model is verified by a MEMS numerical example. The effect of model parameters is studied through sensitivity analysis.

Acknowledgment

This research was funded by the National Natural Science Foundation of China Project (51605083, 12072069); supported by the fundamental research funds for the Central Universities of China Project (N180304022); supported by China Scholarship Council Visiting Scholars Project (201906085037).

References

1. An Z W, Sun D M. Reliability modeling for systems subject to multiple dependent competing failure processes with shock loads above a certain level. Reliability Engineering & System Safety 2017; 157: 129–138, https://doi.org/10.1016/j.ress.2016.08.025.
2. Assaf D, Levikson B. Closure of Phase Type Distributions Under Operations Arising in Reliability Theory. Annals of Probability 1982; 10:265–269, https://doi.org/10.1214/aop/1176993932.
3. Cazorla D, Pérez-Ocón R, Segovia García M. Survival Probabilities for Shock and Wear Models Governed by Phase-Type Distributions. Quality Technology & Quantitative Management 2007; 4: 85–94, https://doi.org/10.1080/16843703.2007.11673136.
4. Che H, Zeng S, Guo J. A reliability model for load-sharing k-out-of-n systems subject to soft and hard failures with dependent workload and shock effects. Eksploatacja i Niezawodnosc – Maintenance and Reliability 2020; 22 (2): 253–264, http://dx.doi.org/10.17531/ein.2020.2.8.
5. Eryilmaz S, Tekin M. Reliability evaluation of a system under a mixed shock model. Journal of Computational and Applied Mathematics 2019; 352: 255–261, https://doi.org/10.1016/j.cam.2018.12.011.
6. Fan M F, Zeng Z G, Zio E, Kang R. Modeling dependent competing failure processes with degradation-shock dependence. Reliability Engineering & System Safety 2017; 165: 422–430, https://doi.org/10.1016/j.ress.2017.05.004.
7. Guo C, Wang W, Guo B, Peng R. Maintenance Optimization for SystemsWith Dependent Competing Risks Using a Copula Function. Eksploatacja i Niezawodnosc – Maintenance and Reliability 2013; 15 (1): 9–17.
8. Hao S H, Yang J, Ma X B, Zhao Y. Reliability modeling for mutually dependent competing failure processes due to degradation and random shocks. Applied Mathematical Modelling 2017; 51: 232–249, https://doi.org/10.1016/j.apm.2017.06.014.
9. He Q M. Fundamentals of Matrix-Analytic Methods. New York: Springer, 2014, https://doi.org/10.1007/978-1-4614-7330-5.
10. Huynh K T, Castro I, Barros A, Berenguer C. Modeling age-based maintenance strategies with minimal repairs for systems subject to competing failure modes due to degradation and shocks. European Journal of Operational Research 2012; 218: 140–151, https://doi.org/10.1016/j.ejor.2011.10.025.
11. Jiang L, Feng Q M, Coit D W. Reliability and Maintenance Modeling for Dependent Competing Failure Processes With Shifting Failure Thresholds. IEEE Transactions on Reliability 2012; 61: 932–948, https://doi.org/10.1109/TR.2012.2221016.
12. Keedy E, Feng Q M. Reliability Analysis and Customized Preventive Maintenance Policies for Stents With Stochastic Dependent Competing Risk Processes. IEEE Transactions on Reliability 2013; 62: 887–897, https://doi.org/10.1109/TR.2013.2285045.
13. Li Z, Kong X. Life behavior of δ-shock model. Statistics & Probability Letters 2007; 77 (6): 577–587, https://doi.org/10.1016/j.spl.2006.08.008.
14. Lin Y H, Li Y F, Zio E. Integrating Random Shocks Into Multi-State Physics Models of Degradation Processes for Component Reliability Assessment. IEEE Transactions on Reliability 2014; 64: 154–166, https://doi.org/10.1109/TR.2014.2354874.
15. Lin Y H, Li Y F, Zio E. Reliability Assessment of Systems Subject to Dependent Degradation Processes and Random Shocks. IIE Transactions 2016; 48: 1072–1085, https://doi.org/10.1080/0740817X.2016.1190481.
16. Lu C, Meeker W. Using Degradation Measures to Estimate a Time-to-Failure Distribution. Technometrics 1993; 35: 161–174, https://doi.org/10.2307/1269661.
17. Lyu H, Zhang X W, Yang Z Y, et al. Reliability Analysis for the Dependent Competing Failure with Wear Model and Its Application to the Turbine and Worm System. IEEE Access 2021 (9): 50265–50280, https://doi.org/10.1109/ACCESS.2021.3062026.
18. Mallor F, Omey E. Shocks, runs and random sums. Journal of Applied Probability 2001; 38: 438–448, https://doi.org/10.1239/jap/996986754.
19. Montoro-Cazorla D, Pérez-Ocón R, Segovia M C. Shock and wear models under policy N using phase-type distributions. Applied Mathematical Modelling 2009; 33 (1): 543–554, https://doi.org/10.1016/j.apm.2007.11.017.
20. Montoro-Cazorla D, Pérez-Ocón R. A reliability system under cumulative shocks governed by a BMAP. Applied Mathematical Modelling 2015; 39 (23): 7620–7629, https://doi.org/10.1016/j.apm.2015.03.066.

21. NI X, Zhao J, Song W, Guo C, Li H. Nonlinear degradation modeling and maintenance policy for a two-stage degradation system based on cumulative damage model. Eksploatacja i Niezawodnosc – Maintenance and Reliability 2016; 18 (2): 171–180, http://dx.doi.org/10.17531/ein.2016.2.3.
22. Ozkut M, Eryilmaz S. Reliability analysis under Marshall–Olkin run shock model. Journal of Computational and Applied Mathematics 2019; 349: 52–59, https://doi.org/10.1016/j.cam.2018.09.022.
23. Peng H, Feng Q M, Coit D W. Reliability and maintenance modeling for systems subject to multiple dependent competing failure processes. IIE Transactions 2010; 43: 12–22, https://doi.org/10.1080/0740817X.2010.491502.
24. Pourhassan MR, Raissi S, Hafezalkotob A. A simulation approach on reliability assessment of complex system subject to stochastic degradation and random shock. Eksploatacja i Niezawodnosc – Maintenance and Reliability 2020; 22 (2): 370–379, http://dx.doi.org/10.17531/ein.2020.2.20.
25. Rafiee K, Feng Q M, Coit D W. Reliability modeling for dependent competing failure processes with changing degradation rate. IIE Transactions 2014; 46: 483–496, https://doi.org/10.1080/0740817X.2013.812270.
26. Rafiee K, Feng Q, Coit D W. Reliability assessment of competing risks with generalized mixed shock models. Reliability Engineering & System Safety 2017; 159: 1–11, https://doi.org/10.1016/j.ress.2016.10.006.
27. Segovia M C, Labeau P E. Reliability of a multi-state system subject to shocks using phase-type distributions. Applied Mathematical Modelling 2013; 37 (7): 4883–4904, https://doi.org/10.1016/j.apm.2012.09.055.
28. Tanner D M, Dugger M. Wear Mechanisms in a Reliability Methodology (Invited). Proceedings of SPIE–The International Society for Optical Engineering 2003; 4980: 22–40, https://doi.org/10.1117/12.476345.
29. Ye Z S, Tang L C, Xu H Y. A distribution-based systems reliability model under extreme shocks and natural degradation. IEEE Transactions on Reliability 2011; 60: 246–256, https://doi.org/10.1109/TR.2010.2103710.
30. Ye Z S, Xie M. Stochastic modelling and analysis of degradation for highly reliable products. Applied Stochastic Models in Business and Industry 2014; 31: 16–32, https://doi.org/10.1002/asmb.2063.
31. Zhang Y, Ma Y, Ouyang L, Liu L. A novel reliability model for multi-component systems subject to multiple dependent competing risks with degradation rate acceleration. Eksploatacja i Niezawodnosc – Maintenance and Reliability 2018; 20 (4): 579–589, http://dx.doi.org/10.17531/ein.2018.4.9.
32. Zhao X, Wang S, Wang X, Cai K. A multi-state shock model with mutative failure patterns. Reliability Engineering & System Safety 2018; 178: 1–11, https://doi.org/10.1016/j.ress.2018.05.014.